Towards measuring the effect of flow in blood T-1 assessed in a flow phantom and in vivo

Hermann, Ingo; Uhrig, Tanja; Chacon-Caldera, Jorge; Akcakaya, Mehmet; Schad, Lothar R.; Weingartner, Sebastian

Important note
To cite this publication, please use the final published version (if applicable).
Please check the document version above.

PAPER • OPEN ACCESS

Towards measuring the effect of flow in blood T_1 assessed in a flow phantom and *in vivo*

View the article online for updates and enhancements.

Physics in Medicine & Biology
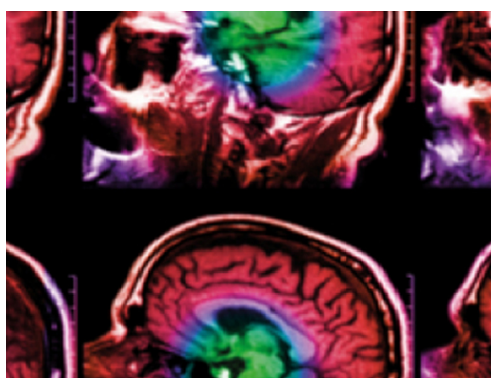
IPEM Institute of Physics and Engineering in Medicine

CrossMark

Towards measuring the effect of flow in blood T_1 assessed in a flow phantom and *in vivo*

Ingo Hermann[1,2], Tanja Uhrig[2], Jorge Chacon-Caldera[2], Mehmet Akçakaya[3,4], Lothar R Schad[2] and Sebastian Weingärtner[1]

[1] Magnetic Resonance Systems Lab, Department of Imaging Physics, Delft University of Technology, Lorentzweg 1, 2628 Delft, Netherlands
[2] Computer Assisted Clinical Medicine, University Medical Center Mannheim, Heidelberg University, Theodor-Kutzer-Ufer 1-3, 68167 Mannheim, Germany
[3] Electrical and Computer Engineering, University of Minnesota, 4-174 Keller Hall 200 Union St. S.E., 55455 Minneapolis, MN, United States of America
[4] Center for Magnetic Resonance Research, University of Minnesota, 2021 6th St SE, 55455 Minneapolis, MN, United States of America

E-mail: ingo.hermann@medma.uni-heidelberg.de, tanja.uhrig@medma.uni-heidelberg.de, jorge.chacon@medma.uni-heidelberg.de, lothar.schad@medma.uni-heidelberg.de and S.Weingartner@tudelft.nl

Keywords: cardiac T_1 mapping, flow velocity dependency, flow phantom, blood T_1

Abstract

Measurement of the blood T_1 time using conventional myocardial T_1 mapping methods has gained clinical significance in the context of extracellular volume (ECV) mapping and synthetic hematocrit (Hct). However, its accuracy is potentially compromised by in-flow of non-inverted/non-saturated spins and in-flow of spins which are not partially saturated from previous imaging pulses.

Bloch simulations were used to analyze various flow effects separately. T_1 measurements of gadolinium doped water were performed using a flow phantom with adjustable flow velocities at 3 T. Additionally, *in vivo* blood T_1 measurements were performed in 6 healthy subjects (26 ± 5 years, 2 female). To study the T_1 time as a function of the instantaneous flow velocity, T_1 times were evaluated in an axial imaging slice of the descending aorta. Velocity encoded cine measurements were performed to quantify the flow velocity throughout the cardiac cycle.

Simulation results show more than 30% loss in accuracy for 10% non-prepared in-flowing spins. However, in- and out-flow to the imaging plane only demonstrated minor impact on the T_1 time. Phantom T_1 times were decreased by up to 200 ms in the flow phantom, due to in-flow of non-prepared spins. High flow velocities cause in-flow of spins that lack partial saturation from the imaging pulses but only lead to negligible T_1 time deviation (less than 30 ms). *In vivo* measurements confirm a substantial variation of the T_1 time depending on the flow velocity. The highest aortic T_1 times are observed at the time point of minimal flow with increased flow velocity leading to reduction of the measured T_1 time by up to 130 ± 49 ms at peak velocity.

In this work we attempt to dissect the effects of flow on T_1 times, by using simulations, well-controlled, simplified phantom setup and the linear flow pattern in the descending aorta *in vivo*.

1. Introduction

Quantitative myocardial tissue characterization has increasingly gained attention in cardiac magnetic resonance imaging (MRI) over the past several years for its ability to non-invasively study the myocardial tissue state (Ferreira *et al* 2014, Hamlin *et al* 2014, Moon *et al* 2013, Messroghli *et al* 2004). Myocardial T_1 mapping is sensitive to changes in the macro-molecular environment and has demonstrated clinical value in various ischemic and non-ischemic cardiomyopathies (Dall'Armellina *et al* 2012, Radenkovic *et al* 2017, Puntmann *et al* 2016). Additionally, extracellular volume (ECV) mapping is widely used as a marker for

fibrotic remodeling of the myocardium in various pathologies (Moon *et al* 2013, Kim *et al* 2017, Haaf *et al* 2016, Messroghli *et al* 2017, Ntusi *et al* 2014). ECV maps are calculated based on native and post-contrast T_1 times in the myocardium and the blood-pool, and are normalized with the hematocrit (Hct). When hematocrit was not measured, or to achieve a more stream-lined process that does not require blood sampling and testing, it has been proposed to calculate a Hct estimate using blood T_1 times in a technique called synthetic Hct (Treibel *et al* 2016). Therefore, ECV and synthetic Hct values are highly dependent on the quality of blood T_1 measurements.

Several cardiac T_1 mapping sequences have been proposed and can be clinically used for native T_1 and ECV mapping (Messroghli *et al* 2004, Chow *et al* 2014, Weingärtner *et al* 2014, Piechnik *et al* 2010, Weingärtner *et al* 2015). Modified Look-Locker inversion recovery (MOLLI) (Messroghli *et al* 2004) is the most widely used method for myocardial T_1 mapping and yields precise T_1 maps but lacks accuracy compared to other T_1 mapping methods (Roujol *et al* 2014). In MOLLI multiple images with different T_1-weightings are acquired following a non-selective inversion pulse. This repeated image acquisition perturbs the magnetization which is corrected for in the reconstruction (Deichmann correction) (Look *et al* 1970, Deichmann *et al* 1992). Saturation recovery single-shot acquisition (SASHA) (Chow *et al* 2014) was proposed as an alternative for T_1 mapping with increased accuracy. In SASHA images are acquired every heartbeat following a non-selective saturation pulse with varying saturation time. Due to a reduced dynamic range and suboptimal sampling of the recovery curve for long T_1 times, SASHA T_1 maps suffer from reduced precision compared with MOLLI (Weingärtner *et al* 2016).

Accuracy and precision of myocardial T_1 mapping are integral to its clinical value and have been thoroughly investigated in several recent studies (Kim *et al* 2017, Haaf *et al* 2016, Roujol *et al* 2014, Weingärtner *et al* 2016, Kellman and Hansen 2014, Cameron *et al* 2018). It was shown that the dominant variability in blood T_1 comes from the biological constituents such as hematocrit, iron, and HDL cholesterol (Rosmini *et al* 2019). However, blood T_1 times often fall out of the range for which myocardial T_1 mapping techniques are validated and multiple confounding mechanisms have been proposed (Choi *et al* 2013, Shang *et al* 2018). In particular it has been suggested that various flow effects compromise T_1 measurement of the blood-pool (Kellman and Hansen 2014). Given the implicit clinical use of blood T_1 times, thorough investigation of the effect of flow is warranted. However, complex flow patterns in the ventricle as well as a multitude of parameters determining the relevant flow hamper the holistic evaluation of this confounder *in vivo*.

In this study, we aim to analyze the impact of certain aspects of flow on T_1 measurements with two commonly used myocardial T_1 mapping techniques in well controlled experimental settings in order to further our understanding of flow as a confounding factor. Bloch simulations are performed to shed light on the relative contribution of different flow effects. These effects are then validated in a controlled flow phantom comprising a peristaltic pump with linear flow. Finally, the combined flow dependency of T_1 measurements is studied *in vivo* by imaging the descending aorta as a proxy, where flow patterns are largely linear and consistently varying across the cardiac cycle.

2. Methods

2.1. Flow effects on blood T_1 measurements

Blood T_1 measurements can be subject to three main flow effects (Kellman and Hansen 2014, Chow *et al* 2014, Cameron *et al* 2018) depending on the myocardial T_1 mapping technique (figure 1).

1. **Non-prepared spins:** In T_1 mapping multiple images are acquired with variable delay following a preparation pulse. During this delay spins that were not subject to the preparation (e.g. far outside the isocenter) can flow into the heart. This increases the signal intensity and therefore decreases the measured T_1 relaxation time.
2. **Beat-to-beat exchange:** For sequences such as MOLLI the same magnetization preparation is read out over multiple heartbeats. Spins flowing into the imaging plane from beat-to-beat are not subject to partial saturation by repeated imaging readouts, but are influenced by one slice selective readout only.
3. **In- and out-flowing spins:** Fast flowing spins that flow into the imaging plane during the readout lead to faster signal regrowth due to partial saturation by one train of imaging pulses.

The Deichmann correction has been introduced to compensate for signal attenuation by continuous FLASH imaging pulses during inversion recovery of static tissue (Deichmann *et al* 1992) and is used in MOLLI to reduce the impact of the imaging readout on the T_1 time. However, in the presence of flow, the correction factor will also be subject to various flow-effects, including reduced effect of the repeated imaging readout and imperfect inversion due to in-flow of non-prepared spins.

Figure 1. Illustration of different flow effects on T_1. Illustration of the three different flow effects corrupting the measurement of blood T_1 times with myocardial T_1 mapping methods. The top panel (a) shows the effect of a T_1 recovery curve over multiple heartbeats, e.g. as seen in MOLLI. In the bottom panel (b) sample magnetization packages (arrows) are depicted during magnetization recovery in various flow scenarios. The signal intensity is encoded by the background shading. The first row shows the recovery in the absence of flow. Rows two to four illustrate the following three flow effects. In-flow of non-prepared spins: An increasing amount of non-prepared spins enter the imaging volume and contribute to faster signal recovery. Beat-to-Beat exchange: Flow between the imaging periods in successive heartbeats eliminates the signal attenuation that is seen with repeated imaging pulses in static tissue. Flow during the imaging readout: Spins that are not affected by previous imaging pulses flow into the imaging volume between two imaging pulses are played and thus mitigate the signal attenuation during an individual readout.

In this study, we try to disentangle the relative contributions of the in-flow of non-prepared spins, beat-to-beat exchange and the flow effect during the imaging readout. We study the effect on the T_1 time, as well as the uncorrected T_1^* for MOLLI and T_1 times calculated with 2- (Kellman *et al* 2014b) and 3-parameter models in SASHA.

2.2. Sequence parameters

T_1 maps were generated using a 5(3 s)3 MOLLI (Kellman *et al* 2012) scheme with and without Deichmann correction (MOLLI T_1/MOLLI T_1^*) for balanced steady-state free precession (bSSFP) readout and for gradient-echo (GRE) readout (MOLLIGRE T_1/MOLLIGRE T_1^*). MOLLI maps are reconstructed by a 3-parameter fit with and without the Deichmann correction. SASHA is reconstructed with 3 and 2 parameter fits (SASHA/SASHA 2P) (Chow *et al* 2014, Kellman *et al* 2014b). Reference T_1 times in the phantom were measured with an inversion recovery (IR) in the absence of flow. T_1 maps were reconstructed with a voxel-wise Levenberg-Marquardt non-linear least-square curve fit implemented in-line on the scanner (Markwardt Craig 1980, Maier *et al* 2019, Lundervold *et al* 2019). All measurements were performed in a 3 T MRI scanner (Magnetom Skyra; Siemens Heathineers, Erlangen, Germany) with a 28-channel receiver coil array and shared the following common imaging parameters: FOV = 240 × 240 mm^2, matrix size (base resolution) = 192 x 192 (1.3 × 1.3 mm), slice thickness = 8 mm, bandwidth = 1085 Hz/px, GRAPPA-factor 2 and partial Fourier 6/8. SSFP imaging was performed with TR/TE = 3.6 ms/1.8 ms and high flip angle of

60°, as recommended in flow and SASHA (Kellman and Hansen 2014), and GRE imaging with TR/TE/α = 2.9 ms/1.7 ms/8°.

Flow velocity measurements were performed with velocity-encoded retrogated cine using TR/TE/α = 53.28 ms/4.37 ms/20°, FOV = 166×240 mm^2, matrix size = 166×240, slice thickness = 8 mm and interpolated phases = 30 and velocity encoding gradient strength $V_{max} = 20$ cm s^{-1} in phantom and $V_{max} = 500$ cm s^{-1} *in vivo*.

2.3. Simulations

We used flow-sensitive Bloch-simulations to determine the relative contribution of the various flow effects for MOLLI and SASHA imaging sequences with bSSFP and GRE readout. All pulse sequences were simulated with the above listed sequence parameters.

For the no flow case, time periods of free relaxation/precession were simulated as

$$\begin{pmatrix} M_x(t+1) \\ M_y(t+1) \\ M_z(t+1) \end{pmatrix} = \begin{pmatrix} E_2 & 0 & 0 \\ 0 & E_2 & 0 \\ 0 & 0 & E_1 \end{pmatrix} \cdot \begin{pmatrix} M_x(t) \\ M_y(t) \\ M_z(t) \end{pmatrix} + \begin{pmatrix} 0 \\ 0 \\ 1 - E_1 \end{pmatrix}, \tag{1}$$

with $E_1 = \exp(t/T_1)$, $E_2 = \exp(t/T_2)$ and the time step t. Center of k-space was chosen to calculate the magnitude with $\sqrt{M_x^2 + M_y^2}$. Imaging and preparation pulses were simulated with corresponding rotation matrices. This magnitude is used for fitting MOLLI and SASHA relaxation curves. Along with the undisturbed relaxation curve without saturation by the readout pulses (no excitation pulses simulated), used as a reference relaxation curve, three different scenarios were simulated: 1) Stationary spins which are repeatedly saturated by the imaging pulses at every heartbeat. 2) Non-prepared spins flowing from the scan periphery into the imaging plane. 3) In-flow of unsaturated spins into the imaging plane during the readout at different flow velocities. For flow simulations, the magnetization vector was split in 1000 magnetization packages $(M_x, M_y, M_z)^T = 1/n \cdot \sum_i^n (M_{x_i}, M_{y_i}, M_{z_i})^T$. In-flow of unsaturated spins is simulated by exchanging magnetization packages with fully relaxed magnetization vectors $(1, 0, 0)^T$. All simulated spins are influenced by only one slice selective imaging readout, as fresh spins are flowing into the imaging plane from beat to beat. Therefore, between heartbeats the magnetization vectors are set to the magnetization of the undisturbed spins. The cardiac cycle was simulated with R-R intervals = 1000 ms and blood relaxation times were simulated as $T_1 = 2000$ ms (Qin *et al* 2010, Varela *et al* 2011, Li *et al* 2017, Liu *et al* 2016) and $T_2 = 200$ ms (Liu *et al* 2016, Chen *et al* 2009). For a given velocity the proportion of unsaturated spins flowing into the imaging plane per time step was calculated as follows:

$$\text{percentage of in-flowing spins per time step} = \frac{\text{flow velocity} \cdot \text{time step}}{\text{slice thickness} \cdot \text{readout duration}}. \tag{2}$$
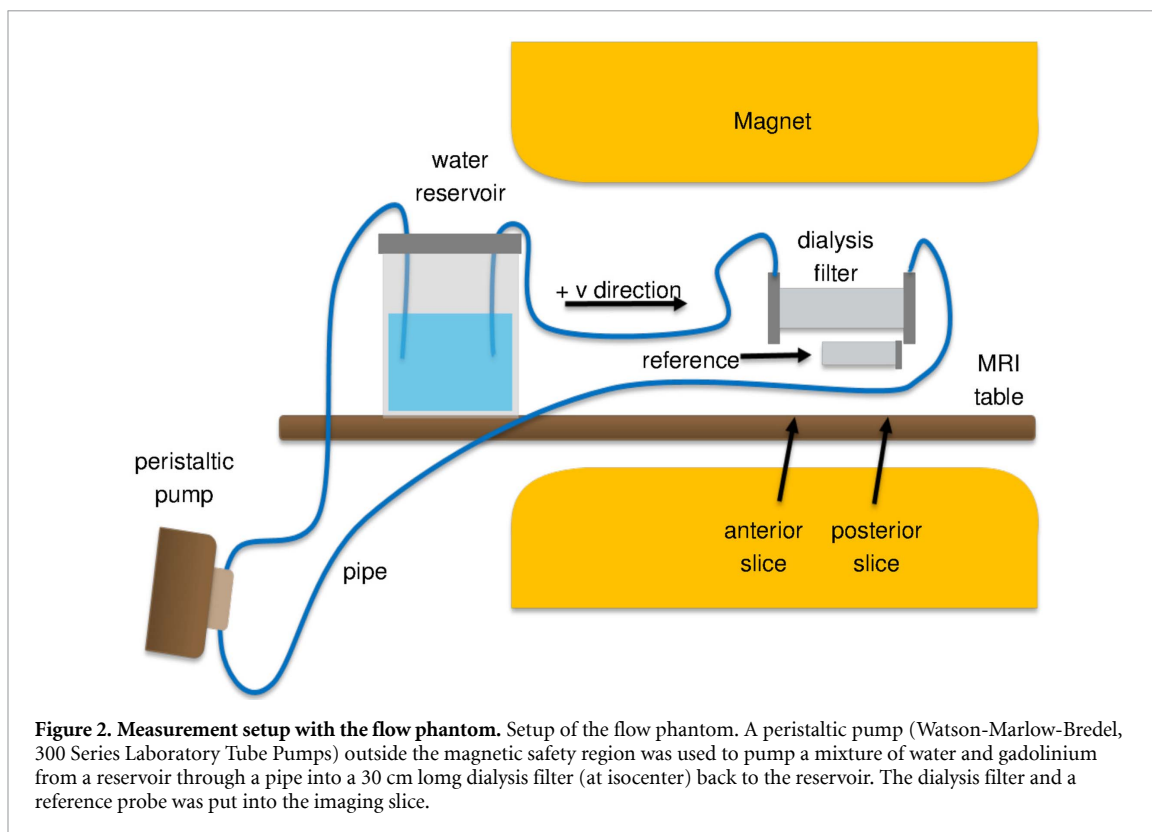
This percentage is used to calculate the amount of magnetization vectors per time step, which are exchanged by the corresponding magnetization vector (all vectors in the magnetization package are the same) from the reference relaxation curve at that time step.

2.4. Phantom experiments

A 30 cm long peristaltic pump (Watson-Marlow-Bredel, 300 Series Laboratory Tube Pumps) was used to circulate gadolinium-doped water from a reservoir outside the scanner bore through a pipe into a dialysis filter (filter with increased diameter, consisting of small fibers). From there the water circulated back outside the bore to the reservoir (figure 2). A dialysis filter with a diameter of 6 cm was used. The dialysis filter and a reference probe (3 cm in diameter) with non-flowing solution were placed in a posterior imaging slice (figure 2). Additionally, imaging was performed in an anterior slice comprising only the dialysis filter. Imaging was performed at five different flow velocities in both flow directions. T_1 measurements were performed using IR, MOLLI T_1/T_1^*, MOLLIGRE T_1/T_1^*, SASHA and SASHA 2P. Additionally, MOLLI and SASHA were performed with a reduced slice thickness of 4 mm to evaluate the flow effect of in-plane saturation. Reference flow velocities were determined by velocity encoded (VENC) cine measurements in the dialysis filter.

2.5. *In vivo* experiments

In vivo measurements were performed in six healthy subjects (26 ± 5 years, 2 female) in a single axial slice positioned approximately five centimeter below the aortic arch. All scans were performed under an IRB-approved protocol and following written, informed consent. T_1 and T_1^* times were calculated and manually drawn region of interests were used to determine mean values and standard deviations in the descending aorta. MOLLI T_1 and T_1^* maps and MOLLIGRE T_1 and T_1^* maps were acquired at various time

Figure 2. Measurement setup with the flow phantom. Setup of the flow phantom. A peristaltic pump (Watson-Marlow-Bredel, 300 Series Laboratory Tube Pumps) outside the magnetic safety region was used to pump a mixture of water and gadolinium from a reservoir through a pipe into a 30 cm lomg dialysis filter (at isocenter) back to the reservoir. The dialysis filter and a reference probe was put into the imaging slice.

points in systole and diastole within the cardiac cycle ranging from 250-800 ms after the R-wave. No SASHA measurements were performed in the aorta as no imaging could be performed during systole. For reference, VENC cine measurements were performed to calculate the blood flow velocity in the aorta throughout the cardiac cycle. Reference measurements of the left ventricular blood pool in a mid-ventricular short axis view (SHAX) were performed with all sequences.

3. Results

3.1. Simulations
Figure 3 demonstrates the effects of the previously described flow-induced phenomena studied in isolation with noise-free Bloch simulations for MOLLI and SASHA.

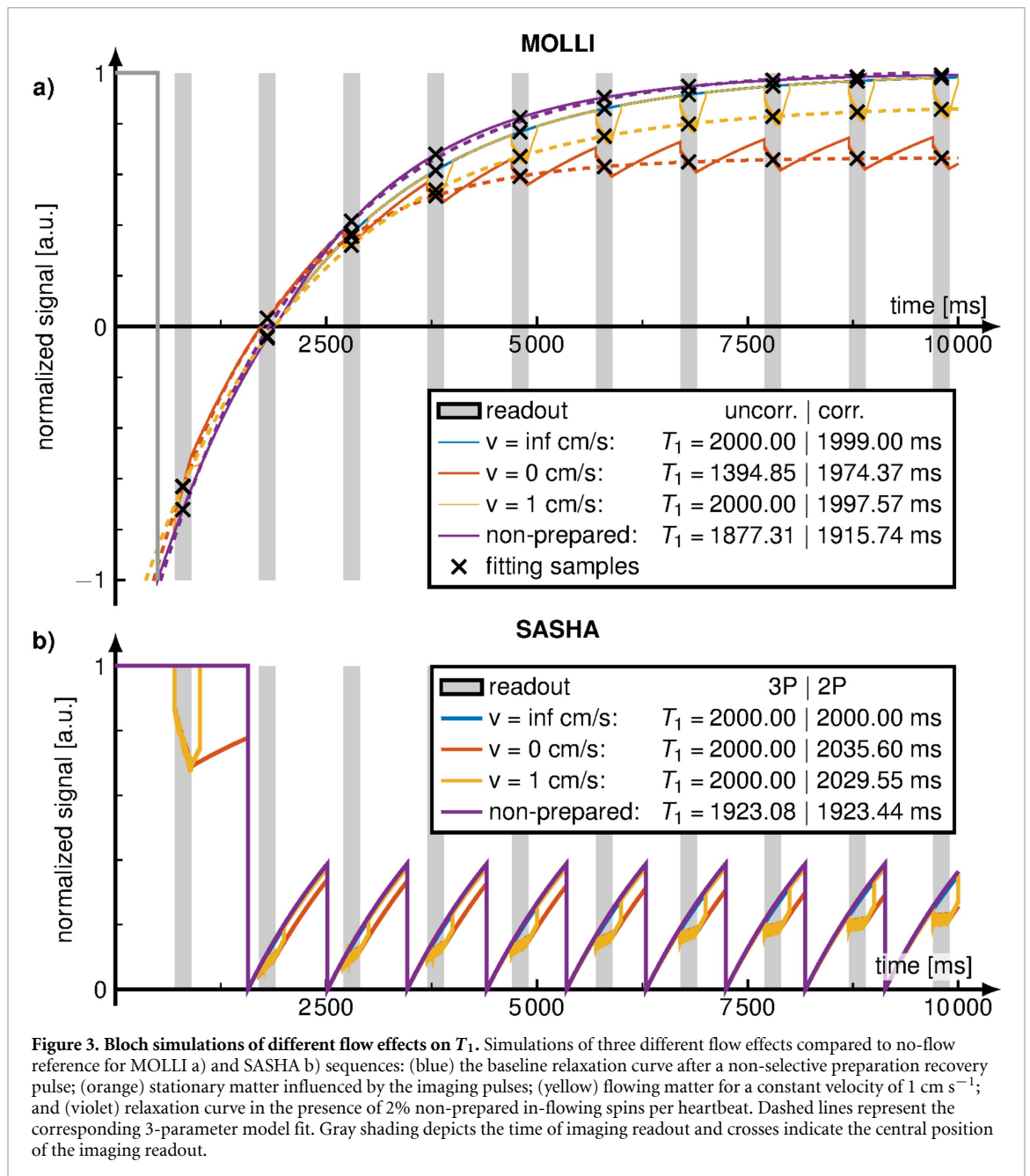#### 3.1.1. In-flow of non-prepared spins
The simulation results in figure 3 show that in-flow of 2% non-prepared spins per heartbeat (purple lines in figure 3) leads to faster recovery and shortened apparent relaxation times. This effect is studied in greater detail for various degrees of in-flow in figure 4. Both MOLLI and SASHA show underestimation, which is increasingly pronounced with higher in-flow. Simulations indicate that for in-flow of 10% non-prepared spins, T_1 time accuracy is compromised by more than 30% and 15% for MOLLI and SASHA, respectively.

3.1.2. Beat-to-beat exchange
Repeated application of imaging pulses leads to signal attenuation across heartbeats in stationary tissue (orange lines in figure 3). However, our results show that even slow flow velocities cause an exchange of the spins between heartbeats (beat-to-beat exchange), such that the imaging signal is just affected by a single set of imaging pulses for any given heartbeat (yellow lines in figure 3). Accordingly, the reduced signal attenuation from previous heartbeats leads to reduced underestimation of T_1 times compared with MOLLI values as commonly obtained in stationary tissue. Without Deichmann correction this leads to a major difference ($\triangle T_1^* > 200$ ms), but was largely mitigated when using Deichmann correction ($\triangle T_1^* < 60$ ms).

3.1.3. In-flow and out-flow during a readout
Flow during the imaging readout leads to further alteration of the magnetization signal as it leads to faster recovery during one imaging readout (i.e. between two imaging pulses, yellow lines in figure 3). This effect is studied in detail in figure 5 at various flow-velocities. Increased T_1 times are observed for SASHA 2P and increased T_1^* times for MOLLI at slow flow up to 5 cm s^{-1}. However, the magnitude of this effect is small

Figure 3. Bloch simulations of different flow effects on T_1. Simulations of three different flow effects compared to no-flow reference for MOLLI a) and SASHA b) sequences: (blue) the baseline relaxation curve after a non-selective preparation recovery pulse; (orange) stationary matter influenced by the imaging pulses; (yellow) flowing matter for a constant velocity of 1 cm s^{-1}; and (violet) relaxation curve in the presence of 2% non-prepared in-flowing spins per heartbeat. Dashed lines represent the corresponding 3-parameter model fit. Gray shading depicts the time of imaging readout and crosses indicate the central position of the imaging readout.

compared to the previously listed contributions ($\sim$1%). Furthermore, the effect is strongly mitigated by using MOLLI with Deichmann correction or SASHA with a 3-parameter fit model. Of note, the consistent offset in T_1 observed with MOLLI is due to incomplete inversion efficiency caused by in-flowing spins. This is not due to its intrinsic well documented errors because we assume that all spins exchange from beat-to-beat and therefore no spins are affected by multiple readouts.

3.2. Phantom experiments

Figure 6 shows the T_1 times measured in the flow phantom for various flow velocities. Negative flow direction for T_1 measurements in the posterior slice and positive flow for the anterior slice, lead to in-flow of spins from the reservoir outside the scanner bore, into the imaging plane. For these regimes (blue shaded area, figures 6(a) and (b)) T_1 times decrease by up to 125 ms with a decrease of 25 ms per 1 cm s^{-1} for SASHA/SASHA 2P and up to 250 ms with a decrease of 50 ms per 1 cm s^{-1} for MOLLI/MOLLIGRE with and without Deichmann correction. The highest deviation is observed at the largest velocity amplitude ($v \sim 5$ cm s^{-1}).

For absolute flow-velocities larger than $1 - 1.5$ cm s^{-1} all spins from the imaging readout can be assumed to have left the imaging plane during one heartbeat (beat-to-beat exchange). However, for slow absolute flow velocities (-1.5 cm s^{-1} to 1.5 cm s^{-1}) a varying degree of beat-to-beat exchange can affect the
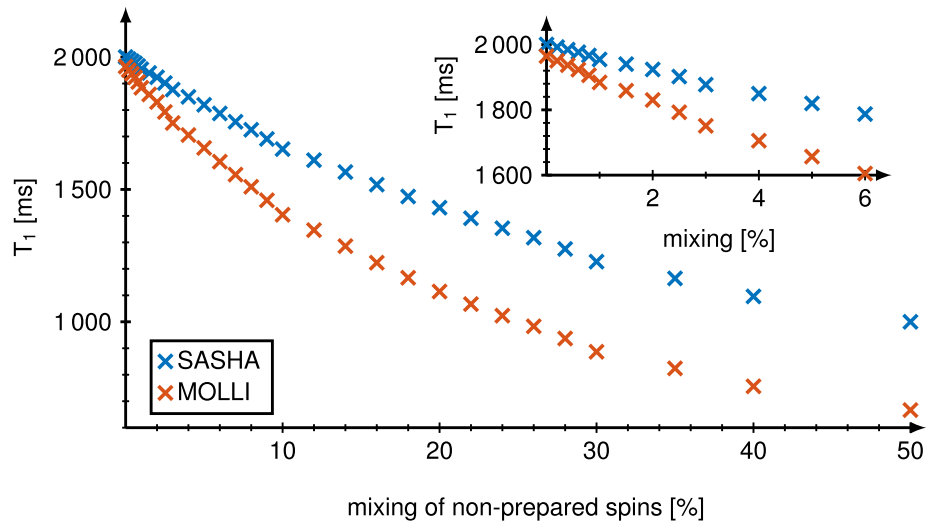
Figure 4. Bloch simulations of non-prepared inflowing spins. T_1 time as a function of the amount of in-flowing non-prepared spins in percentage per heartbeat for SASHA (blue) and MOLLI T_1^*, T_1 (orange). Of note, the time for in-flow of non-prepared spins is substantially shorter for SASHA due to repeated magnetization saturation in every heartbeat.
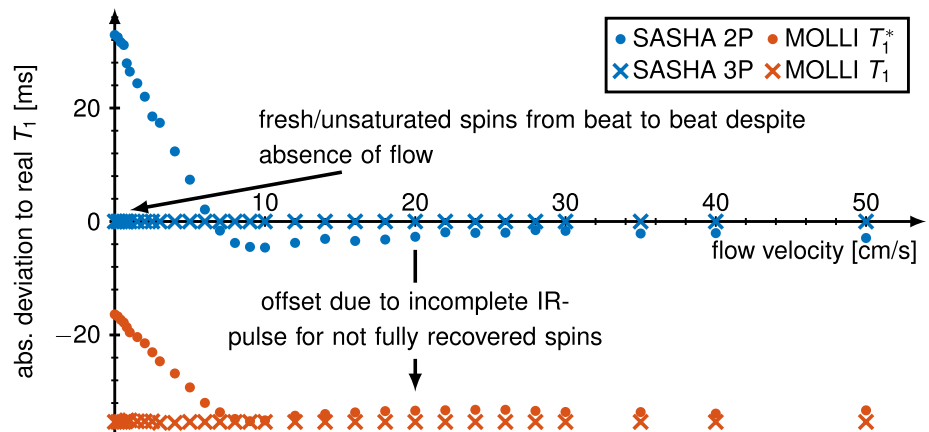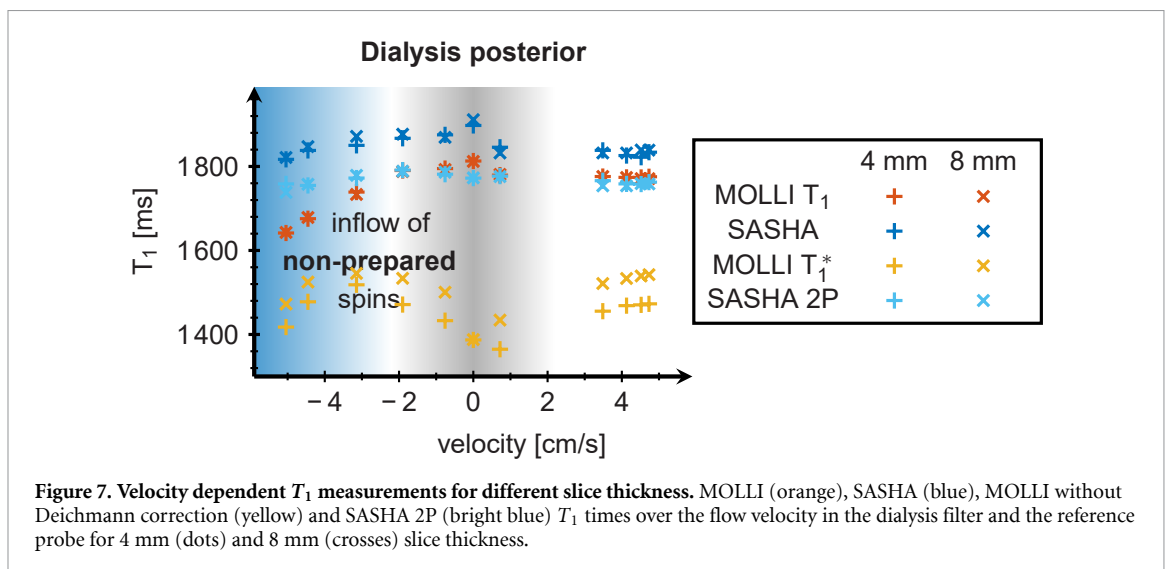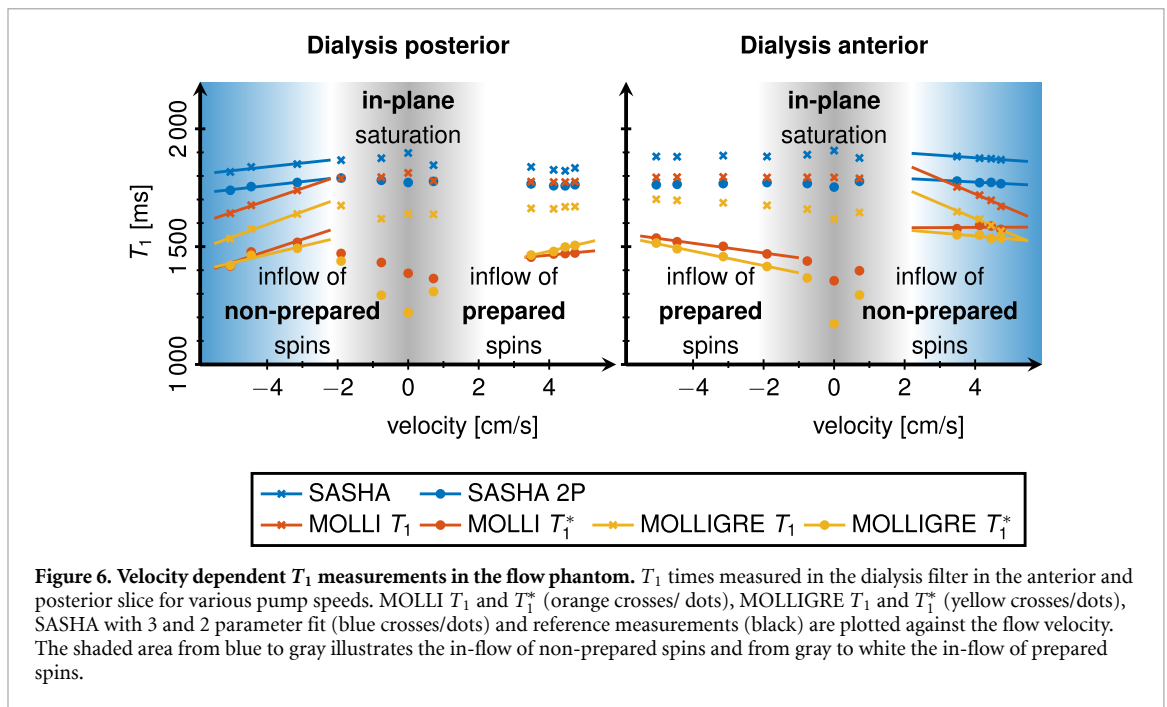

Figure 5. Bloch simulations of partial saturation by imaging pulses. T_1 time for in-flowing and out-flowing spins during a single readout for SASHA (blue) and MOLLI T_1^*, T_1 (orange). Simulations were performed under the assumption that irrespective of the flow velocity, spins are fully exchanged from beat-to-beat.

T_1 times. In this regime (gray shaded area, figures 6(a) and (b)) MOLLIs without Deichmann correction show a symmetrical peak for around $v = 0$ cm s^{-1}, leading to T_1^* deviation of more than 200 ms. This contribution is largely eliminated when using a Deichmann correction. SASHA shows only minor variation in this flow regime, which is expected as beat-to-beat exchange does not affect the SASHA signal due to the repeated saturation.

For large flow-velocities in the opposite flow direction, mostly prepared spins are flowing into the imaging plane. In this regime (white shaded area, figure 6(a) and (b)) varying amount of in-flow/out-flow during the readout is expected to be the dominant effect inducing flow susceptibility. MOLLI without Deichmann correction shows sensitivity to this flow effect, with increasing T_1^* times for increasing flow magnitude. However, the effect is largely mitigated using Deichmann correction. No sensitivity to flow for SASHA or SASHA 2P can be discerned from the noise level in this regime. These findings are corroborated by the results of measurements with different slice thickness (figure 7), which also leads to difference in in-flow/out-flow during the readout. All T_1 methods yield excellent agreement for measurements at 4 mm and 8 mm slice thickness (absolute deviation less than 20 ms), except MOLLI without Deichmann correction. Substantial variation up to 80 ms is observed in the presence of flow, but excellent agreement is shown for the minimal flow case (deviation less than 26 ms).

In the reference probe T_1 maps of SASHA/SASHA 2P achieved good agreement with IR yielding deviations less than 6% whereas MOLLI T_1/MOLLI T_1^* underestimated the T_1 time of approximately 15%. MOLLIGRE underestimated the T_1 time by almost 20% and MOLLIGRE T_1^* by 28%. All measurements

Figure 6. Velocity dependent T_1 measurements in the flow phantom. T_1 times measured in the dialysis filter in the anterior and posterior slice for various pump speeds. MOLLI T_1 and T_1^* (orange crosses/ dots), MOLLIGRE T_1 and T_1^* (yellow crosses/dots), SASHA with 3 and 2 parameter fit (blue crosses/dots) and reference measurements (black) are plotted against the flow velocity. The shaded area from blue to gray illustrates the in-flow of non-prepared spins and from gray to white the in-flow of prepared spins.

Figure 7. Velocity dependent T_1 measurements for different slice thickness. MOLLI (orange), SASHA (blue), MOLLI without Deichmann correction (yellow) and SASHA 2P (bright blue) T_1 times over the flow velocity in the dialysis filter and the reference probe for 4 mm (dots) and 8 mm (crosses) slice thickness.

resulted in standard deviations of less than 50 ms for SASHA, SASHA 2P, MOLLI, MOLLIGRE and less than 100 ms for MOLLI T_1^* and MOLLIGRE T_1^*.

3.3. *In vivo* experiments

MOLLI T_1 maps were generated for an axial cross-section of the aorta at various time points throughout the cardiac cycle. Across all subjects, peak velocities up to 120 cm s^{-1} were measured with an average peak velocity of 77 ± 24 cm s^{-1}. Figure 8 depicts the flow velocity and blood T_1 times as a function of time within the cardiac cycle of one healthy subject. A summary of T_1 times in the absence of flow and during peak velocity are given in table 1. T_1 times increased with decreasing velocity with differences up to 186 ms. Across all subjects MOLLI and MOLLIGRE measured during the diastole (slow flow) resulted in T_1 times comparable to the left ventricle in the SHAX measurement. Mean differences of T_1 times between peak flow and time point of minimal flow, and their corresponding standard deviations were 163 ± 57 ms for MOLLI, 115 ± 41 ms for MOLLIGRE, 424 ± 192 ms for MOLLI T_1^* and 362 ± 181 ms for MOLLIGRE T_1^*. T_1 maps with Deichmann correction were more precise with standard deviations in the aorta of 107–252 ms over the cardiac cycle. Without Deichmann correction standard deviations vary from 203 ms for MOLLI up to 726 ms for MOLLIGRE respectively.
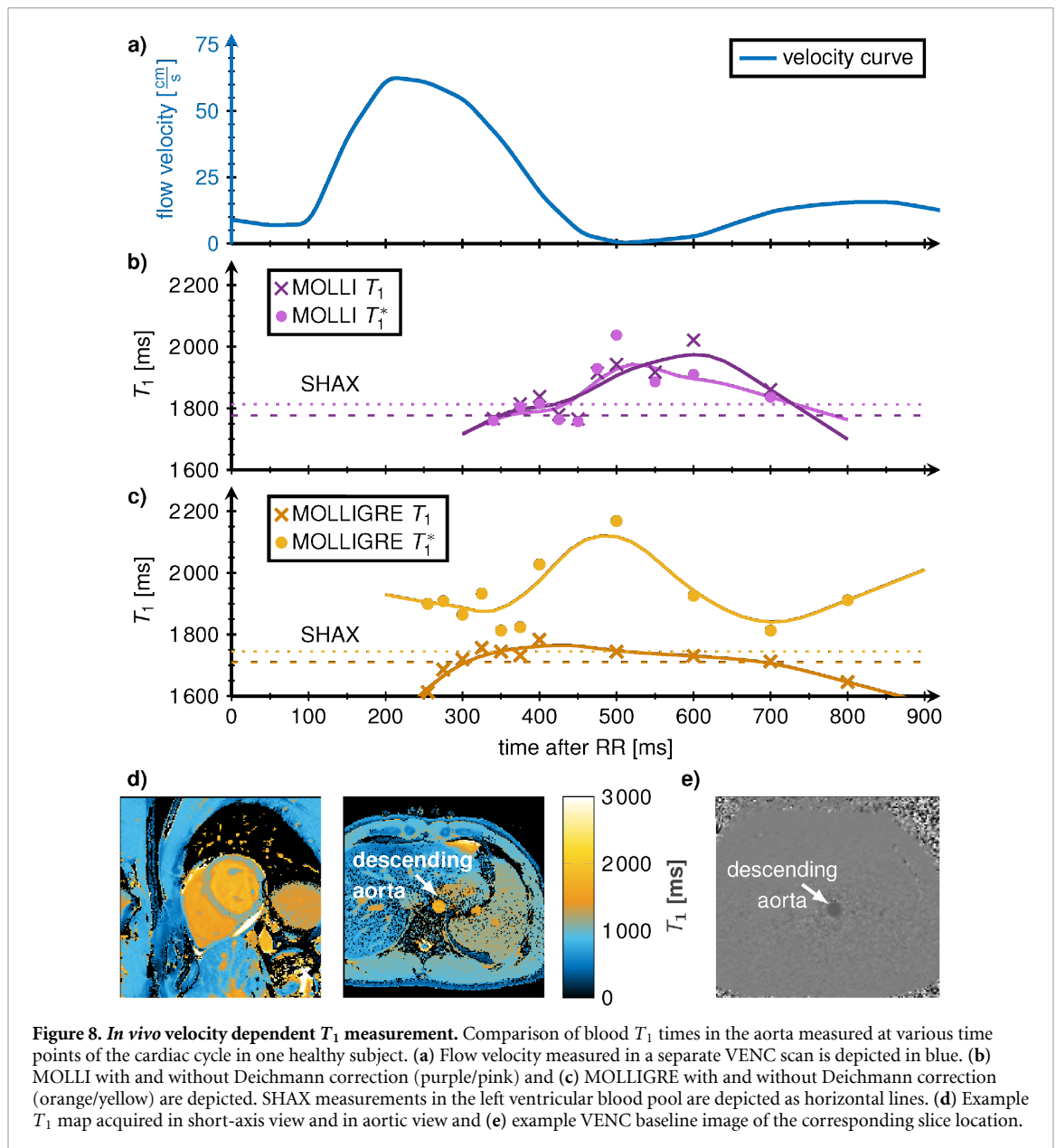
Figure 8. *In vivo* **velocity dependent T_1 measurement.** Comparison of blood T_1 times in the aorta measured at various time points of the cardiac cycle in one healthy subject. (**a**) Flow velocity measured in a separate VENC scan is depicted in blue. (**b**) MOLLI with and without Deichmann correction (purple/pink) and (**c**) MOLLIGRE with and without Deichmann correction (orange/yellow) are depicted. SHAX measurements in the left ventricular blood pool are depicted as horizontal lines. (**d**) Example T_1 map acquired in short-axis view and in aortic view and (**e**) example VENC baseline image of the corresponding slice location.

4. Discussion

In this study we performed flow-dependent T_1 measurements using MOLLI and SASHA to evaluate different contributions of flow effects with simulations, phantom and *in vivo* measurements. Three flow effects were studied to play a role in blood T_1 measurements:

- In-flow of non-prepared spins from outside the scanner bore increase the signal magnetization and induce a faster T_1 relaxation.
- Sufficiently fast spins flowing outside the imaging plane from heartbeat to heartbeat eliminate the in-plane saturation effect and can result in decreased underestimation of MOLLI T_1 times compared with stationary tissue. However, the effect is small when Deichmann correction is used.
- Spins which flow inside and outside the imaging plane during one readout increase the signal intensity. This leads to higher T_1^* for MOLLI but was mitigated when using Deichmann correction and did not affect SASHA.

Simulations and phantom measurements indicate that in-flow of non-prepared spins is the dominant flow effect. Our results show that this can lead to substantial deviations in the T_1 time, especially for large fractions of in-flowing non-prepared spins. The effect on SASHA T_1 times was substantially smaller

Table 1. **Tabular of all *in vivo* blood T_1 values.** Aortic blood T_1 times for MOLLI and MOLLIGRE with and without Deichmann correction for six healthy subjects. T_1 times for the time points in the cardiac cycle with no and maximum flow velocities are provided.

subject, gender	Sequence	Deichmann correction	speed [cm s^{-1}]	min. flow T_1 [ms]	peak flow T_1 [ms]	diff. T_1 [ms]
1, f	MOLLI	on	76	1917±107	1759±66	158
		off		2126±384	1806±231	319
	MOLLIGRE	on		1838±375	1664±170	174
		off		2456±825	2041±649	415
2, m	MOLLI	on	64	1809 ± 252	1751 ± 121	58
		off		1898 ± 726	1965 ± 386	67
	MOLLIGRE	on		1757 ± 186	1737 ± 133	20
		off		2056 ± 843	1853 ± 656	203
3, m	MOLLI	on	63	1868 ± 123	1681 ± 209	186
		off		1839 ± 366	1159 ± 785	680
	MOLLIGRE	on		1757 ± 186	1737 ± 133	20
		off		2056 ± 843	1853 ± 656	203
4, f	MOLLI	on	54	1973 ± 222	1817 ± 424	156
		off		1921 ± 562	1430 ± 951	490
	MOLLIGRE	on		1930 ± 99	1844 ± 204	86
		off		2150 ± 330	1846 ± 675	304
5, m	MOLLI	on	87	1662 ± 162	1580 ± 410	82
		off		1607 ± 207	1039 ± 725	568
	MOLLIGRE	on		1639 ± 123	1552 ± 185	87
		off		1731 ± 457	1382 ± 627	349
6, m	MOLLI	on	120	1792 ± 174	1650 ± 301	142
		off		1638 ± 203	1297 ± 631	342
	MOLLIGRE	on		1734 ± 213	1650 ± 294	84
		off		1663 ± 452	1445 ± 671	218

compared with MOLLI because a non-selective saturation pulse erases the magnetization every heartbeat. For MOLLI T_1 times in-flow of non-prepared spins exacerbates T_1 underestimation.

The amount of non-prepared spins in blood T_1 measurements depends on a number of system and subject specific patterns. Besides the properties of the individual's circulation, the pulse type, the B_1^+ and B_0 inhomogeneity off the isocenter determine the reach of the preparation pulse. For the commonly used tan/tanh pulse as proposed by Kellman *et al* (Kellman *et al* 2014a) inversion efficiency of less than 0.5 is observed for around 1/3 of the peak B_1 amplitude. Our used body coil with 55 cm length has a 50% B_1 amplitude decrease 15 cm away from the iso-center. Therefore, spins outside the bore are negligibly influenced by the non-selective preparation pulses. Blood takes about 20 seconds for one circulation throughout the entire vascular system. Hence, throughout the inversion span of a typical MOLLI sequence, which reaches up to 5 seconds, non-negligible amounts of un-prepared spins can be expected to flow into the imaging plane.

The impact of the other two flow effects was relatively small compared to in-flow of non-prepared spins. Furthermore, the impact of the beat-to-beat exchange and the flow during the imaging readout were effectively mitigated using the Deichmann correction for MOLLI or using SASHA. We performed MOLLI experiments with and without Deichmann correction to fully understand the cause of flow susceptibility. Our simulations also showed that for increasing T_1 all flow effects increase. However, simulations and phantom measurements demonstrated higher resilience to flow effects in MOLLI with Deichmann correction, despite the known discrepancy between the assumptions underlying the correction and the MOLLI sequence (Shang *et al* 2018).

The effect of flow on the blood T_1 time plays a role in the calculation of ECV. However, our results indicate that the flow effects are more pronounced for longer T_1 times. The ECV calculation is more susceptible to changes in the post-contrast T_1 times, and thus shows stronger resilience to flow induced variations. Given the simulated effects from figure 4, errors about 5% can be expected for ECV. However, the synthetic Hct is inversely proportional to the native blood T1 times. Thus, decreasing blood T1 times increases the Hct. With flow induced T1 deviations of up to 20% synthetic Hct may vary by up to 17%. Hence, when using synthetic Hct for ECV calculation this error propagates to the ECV value linearly.

In vivo measurements confirm the flow effect of decreasing T_1 times by increasing flow velocity in the descending aorta. Due to the relatively high standard deviation *in vivo*, in-flow and out-flow of spins during a readout as observed in phantom can be assumed to be negligible. Flow susceptibility due to varying degrees of beat-to-beat exchange can also be assumed to be negligible due to the high ejection fraction in the aorta.

Accordingly, our *in vivo* results in the aorta suggest a strong impact of in-flow of non-prepared spins on the T_1 time, indicating potential *in vivo* contribution of the dominant effect observed in phantom and simulations.

MOLLI T_1 mapping is well known to be susceptible to variations in prescribed or actual flip-angles (Cooper *et al* 2014, Kellman *et al* 2013). In-flow of spins during the readout, also impacts the amount of signal attenuation in tissue, although with different underlying principles. Therefore, we studied the contribution of flow to MOLLI T_1 times. Simulations suggested that the Deichmann correction is highly effective in mitigating the effects of variable signal saturation in the presence of flow. To further confirm this result, phantom experiments were conducted in a slow flow regime. In these experiments, in-flow during the readout is expected to affect T_1 times independent of the flow direction thus constituting a symmetrical peak. While this effect was observed the relative contribution compared with in-flow of non-prepared spins was almost negligible after Deichmann correction. This was further confirmed in scans with decreased slice thickness, which leads to increased in-flow/out-flow during the readout for a given flow velocity. As shown in our simulations, theoretically there is no need for correcting with Deichmann for sufficient fast flow. Nevertheless, our phantom measurements resulted in decreased T_1 times with higher standard deviations compared with using the Deichmann correction.

SASHA T_1 mapping showed substantially lower susceptibility to flow effects. However, residual changes in T_1 times were induced, primarily due to the in-flow of non-prepared spins. In simulations and phantom experiments, constant flow velocities were simulated throughout the heartbeat. However, *in vivo* in-flow of non-prepared spins is largely restricted to the systolic phase, potentially leading to even smaller flow susceptibility in the T_1 measurement. However, no SASHA imaging could be performed to study the flow effect in the aorta directly, as SASHA is incompatible with a variable readout timing with respect to the cardiac cycle.

Overall, our results demonstrate that under controlled conditions the T_1 times of moving fluids can be strongly dependent on flow velocities. These results are obtained in simplified and well controlled conditions. However, a multitude of factors likely determines the effect size on left ventriclualr blood T_1 as commonly performed. While this limits the feasibility, our results confirm the literature postulation that in-flow of non saturated spins is a potential confounder in blood T_1 measurement. The total in-flow and the flow velocity depends on a number of physiological parameters. The total stroke volume determines how much potentially non-prepared spins can flow in from the periphery. The patient size can affect the amount of blood in the periphery that is potentially not completely prepared. Ejection fraction can also be a confounding factor for blood T_1 measurements as this can variably affect the amount of beat-to-beat exchange. Hence, our results suggest that the use of blood T_1 as an independent parameter warrants careful consideration. Thorough control for flow determining physiology might potentially help to reduce variability (Becker *et al* 2019, Collis *et al* 2001, Barone-Rochette *et al* 2013). Due to the important role of blood T_1 in ECV mapping and due to its recent use in synthetic Hct numerous clinical studies evaluated cardiomyopathies based on blood T_1 based quantities (Haaf *et al* 2016, Kellman *et al* 2012, Ugander *et al* 2012, Ntusi *et al* 2014, Cameron *et al* 2018, Messroghli *et al* 2017, Moon *et al* 2013). As the effects observed in quantitative myocardial tissue characterization are often small it is paramount to understand potential confounders. Our results indicate that measurements in patients with largely varying flow-determining physiology could lead to increased variability in blood T_1 based biomarkers. This can potentially hamper the identification of pathological changes.

This study has several limitations. A number of simplifications had to be made in order to systematically analyze the impact of flow on myocardial T_1 mapping. These simplification limit the direct feasibility of the results to the measurements of blood T_1 times in the left ventricle. Firstly, the phantom setup was a simplified approach to measure the effects of different flow patterns in isolation. The reservoir was put outside the bore to create an environment where non-prepared spins flow into the imaging plane. However, the fraction of spins that is poorly polarized is likely smaller *in vivo* than as in this setting. Imaging of the descending aorta was performed as an *in vivo* model with controllable instantaneous flow velocities. However, different and more variable flow patterns are characteristic for the left ventricle potentially giving rise to different flow response of the T_1 time. A difference in local flow-patterns can potentially have minor impact on the effects of in-/out-flow during the readout. In our simulations we assumed 100% inversion efficiency with a rectangular slice profile without taking the distribution of flip angles into account. However, in-plane saturation only demonstrated minor effects on blood T1 times. For this reason we suspect that a distribution of flip angles as a result of the slice profile will only play a minor role. However, given our results indicate overall negligible contribution of this flow effect a detailed analysis of turbulent flow in dedicated phantoms or the ventricles might not be required.

5. Conclusion

T_1 times in moving fluids such as blood obtained with commonly used T_1 mapping techniques can be susceptible to flow-effects. In our simplified model analysis, we found the most significant flow effect due to in-flow of non-prepared spins. Other flow-induced effects showed minor impact and were well compensated for using either a Deichmann correction for MOLLI or SASHA. Overall, SASHA proved to be less prone to flow effects as the magnetization is saturated in every heartbeat compared with MOLLI, where a single inversion pulse spans up to five heartbeats. These results are suggestive that in-flow of non saturated spins could potentially be detrimental to blood T_1 measurements with potential implications for analysis of ECV and synthetic Hct, but thorough clinical investigation of the impact is warranted.

References

Ferreira V M, Piechnik S K, Robson M D, Neubauer S and Karamitsos T D 2014 Myocardial tissue characterization by magnetic resonance imaging: novel applications of T1 and T2 mapping *J. Thoracic Imaging* **29** 147–54

Hamlin S A, Henry T S, Little B P, Lerakis S and Stillman A E 2014 Mapping the future of cardiac MR imaging: case-based review of T1 and T2 mapping techniques *RadioGraphics* **34** 1594–1611

Moon J C *et al* 2013 Myocardial T1 mapping and extracellular volume quantification: a Society for Cardiovascular Magnetic Resonance (SCMR) and CMR Working Group of the European Society of Cardiology consensus statement *J. Cardiovasc. Magn. Reson.* **15** 92

Messroghli D R, Radjenovic A, Kozerke S, Higgins D M, Sivananthan M U and Ridgway J P 2004 Modified look-locker inversion recovery (MOLLI) for high-resolution T1 mapping of the heart *Magn. Reson. Med.* **52** 141–6

Dall'Armellina E, Piechnik S K, Ferreira V M and Si Q L 2012 Cardiovascular magnetic resonance by non contrast T1-mapping allows assessment of severity of injury in acute myocardial infarction *J. Cardiovasc. Magn. Reson.* **14** 15

Radenkovic D, Weingärtner S, Ricketts L, Moon J C and Captur G 2017 T1 mapping in cardiac MRI *Heart Fail. Rev.* **22** 415–30

Puntmann V O, Peker E, Chandrashekhar Y and Nagel E 2016 T1 mapping in characterizing myocardial disease a comprehensive review *Circ. Res.* **119** 277–99

Kim P *et al* 2017 Myocardial T1 and T2 mapping: techniques and clinical applications *Korean J. Radiol.* **18** 113–31

Haaf P, Garg P, Messroghli D R, Broadbent D A, Greenwood J P and Plein S 2016 Cardiac T1 mapping and extracellular volume (ECV) in clinical practice: a comprehensive review *J. Cardiovasc. Magn. Reson.* **18** 89

Messroghli D R *et al* 2017 Clinical recommendations for cardiovascular magnetic resonance mapping of T1, T2, T2* and extracellular volume: a consensus statement by the Society for Cardiovascular Magnetic Resonance (SCMR) endorsed by the European Association for Cardiovascular Imaging (EACVI) *J. Cardiovasc. Magn. Reson.* **19** 75

Ntusi N A *et al* 2014 Subclinical myocardial inflammation and diffuse fibrosis are common in systemic sclerosis—a clinical study using myocardial T1-mapping and extracellular volume quantification *J. Cardiovasc. Magn. Reson.* **16** 21

Treibel T A *et al* 2016 Automatic measurement of the myocardial interstitium: synthetic extracellular volume quantification without hematocrit sampling *JACC: Cardiovasc. Imaging* **9** 54–63

Chow K, Flewitt J A, Green J D, Pagano J J, Friedrich M G and Thompson R B 2014 Saturation recovery single shot acquisition (SASHA) for myocardial T1 mapping *Magn. Reson. Med.* **71** 2082–95

Weingärtner S, Akçakaya M, Basha T, Kissinger K V, Goddu B, Berg S, Manning W J and Nezafat R 2014 Combined saturation/inversion recovery sequences for improved evaluation of scar and diffuse fibrosis in patients with arrhythmia or heart rate variability *Magn. Reson. Med.* **71** 1024–34

Piechnik S K, Ferreira V M, Dall'Armellina E, Cochlin L E, Greiser A, Neubauer S and Robson M D 2010 Shortened modified look-locker inversion recovery (ShMOLLI) for clinical myocardial T1-mapping at 1.5 and 3 T within a 9 heartbeat breathhold *J. Cardiovasc. Magn. Reson.* **12** 69

Weingärtner S, Roujol S, Akçakaya M, Basha T A and Nezafat R 2015 Free-breathing multislice native myocardial T1 mapping using the slice-interleaved T1 (stone) sequence *Magn. Reson. Med.* **74** 115–24

Roujol S *et al* 2014 Accuracy, precision and reproducibility of four T1 mapping sequences: a head-to-head comparison of MOLLI, ShMOLLI, SASHA, and SAPPHIRE *Radiology* **272** 683–9

Look D C and Locker D R 1970 Time saving in measurement of NMR and EPR relaxation times *Rev. Sci. Instrum.* **41** 250–1

Deichmann R and Haase A 1992 Quantification of T1 values by snapshot-flash NMR imaging *J. Magn. Reson.* **96** 608–12

Weingärtner S, Meßner N M, Budjan J, Loßnitzer D, Mattler U, Papavassiliu T, Zöllner F G and Schad L R 2016 Myocardial T1-mapping at 3T using saturation-recovery: reference values, precision and comparison with MOLLI *J. Cardiovasc. Magn. Reson.* **18** 84

Kellman P and Hansen M S 2014 T1-mapping in the heart: accuracy and precision *J. Cardiovasc. Magn. Reson.* **16** 2

Cameron D, Vassiliou V S, Higgins D M and Gatehouse P D 2018 Towards accurate and precise T1 and extracellular volume mapping in the myocardium: a guide to current pitfalls and their solutions *Magn. Reson. Mater. Phys. Biol. Med.* **31** 143–163

Rosmini S *et al* 2019 The effect of blood composition on T1 mapping *JACC: Cardiovasc. Imaging* **12** 1888–90

Choi E-Y *et al* 2013 Correction with blood T1 is essential when measuring post-contrast myocardial T1 value in patients with acute myocardial infarction *J. Cardiovasc. Magn. Reson.* **15** 11

Shang Y, Zhang X, Zhou X, Greiser A, Zhou Z, Li D and Wang J 2018 Blood T1* correction increases accuracy of extracellular volume measurements using 3T cardiovascular magnetic resonance: Comparison of T1 and T1* maps *Sci. Rep.* **8** 2045–322

Kellman P, Xue H, Chow K, Spottiswoode B S, Arai A E and Thompson R B 2014 Optimized saturation recovery protocols for T1-mapping in the heart: influence of sampling strategies on precision *J. Cardiovasc. Magn. Reson.* **16** 55

Kellman P, Wilson J R, Xue H, Ugander M and Arai A E 2012 Extracellular volume fraction mapping in the myocardium, part 1: evaluation of an automated method *J. Cardiovasc. Magn. Reson.* **14** 63

Markwardt Craig (1980) MPFIT: A MINPACK-1 Least Squares Fitting Library in C [Accessed: April 2019] www.physics.wisc.edu/texttildelow craigm/idl/cmpfit.html

Maier A, Syben C, Lasser T and Riess C 2019 A gentle introduction to deep learning in medical image processing *Z. Med. Phys.* **29** 96–101

Lundervold A S and Lundervold A 2019 An overview of deep learning in medical imaging focusing on MRI *Z. Med. Phys.* **29** 102–27

Qin Q, Strouse J J and van Zijl P C M 2010 Fast measurement of blood T1 in the human jugular vein at 3 Tesla *Magn. Reson. Med.* **65** 1297–304

Varela M, Hajnal J V, Petersen E T, Golay X, Merchant N and Larkman D J 2011 A method for rapid in vivo measurement of blood T1 *NMR Biomed.* **24** 80–8

Li W, Liu P, Lu H, Strouse J J, van Zijl P C M and Qin Q 2017 Fast measurement of blood T1 in the human carotid artery at 3T: accuracy, precision and reproducibility *Magn. Reson. Med.* **77** 2296–302

Liu P, Chalak L F, Krishnamurthy L C, Mir I, Peng S-l Huang H and Lu H 2016 T1 and T2 values of human neonatal blood at 3 Tesla: dependence on hematocrit, oxygenation and temperature *Magn. Reson. Med.* **75** 1730–5

Chen J J and Pike G B 2009 Human whole blood T2 relaxometry at 3 Tesla *Magn. Reson. Med.* **61** 249–54

Kellman P, Herzka D A and Hansen M S 2014 Adiabatic inversion pulses for myocardial T1 mapping *Magn. Reson. Med.* **71** 1428–34

Cooper M A, Nguyen T D, Spincemaille P, Prince M R, Weinsaft J W and Wang Y 2014 How accurate is MOLLI T1 mapping in vivo? Validation by spin echo methods *PLOS ONE* **9** e107327

Kellman P, Herzka D A, Arai A E and Hansen M S 2013 Influence of off-resonance in myocardial T1-mapping using SSFP based MOLLI method *J. Cardiovasc. Magn. Reson.* **15** 63

Becker H, Wattenberg M, Barth P, Laser K T, Burchert W and Krperich H 2019 Impact of different respiratory monitoring techniques on respiration-dependent stroke-volume measurements assessed by real-time magnetic resonance imaging *Z. Med. Phys.* **29** 349–58

Collis T, Devereux R B, Roman M J, de Simone G, Yeh J-L, Howard B V, Fabsitz R R and Welty T K 2001 Relations of stroke volume and cardiac output to body composition *Circulation* **103** 820–5

Barone-Rochette G *et al* 2013 Aortic valve area, stroke volume, left ventricular hypertrophy, remodeling, and fibrosis in aortic stenosis assessed by cardiac magnetic resonance imaging *Cir.: Cardiovasc. Imaging* **6** 1009–17

Ugander M *et al* 2012 Extracellular volume imaging by magnetic resonance imaging provides insights into overt and sub-clinical myocardial pathology *Eur. Heart J.* **33** 1268–78